

Scaling investigation of renormalized correlation functions in $O(a)$ improved quenched lattice QCD



Jochen Heitger

Deutsches Elektronen-Synchrotron, DESY Zeuthen
Platanenallee 6, D-15738 Zeuthen, Germany

Abstract

We present a scaling investigation of some correlation functions in $O(a)$ improved quenched lattice QCD. In particular, as one observable the renormalized PCAC quark mass is considered. Others are constructed such that they become the vector meson mass and the pseudoscalar meson decay constant when the volume is large. For the present discussion we remain in intermediate volume, $(0.75^3 \times 1.5) \text{ fm}^4$ with Schrödinger functional boundary conditions. By fixing the 'pion mass' and the spatial lattice size in units of the hadronic scale r_0 , we simulated four lattices with resolutions ranging from 0.1 fm to 0.05 fm and performed the extrapolation to the continuum limit. The maximal scaling violation found in the improved theory is a $\sim 6\%$ effect at $a \simeq 0.1$ fm.

1 Introduction

One of the major drawbacks in the standard formulation of lattice QCD, induced by the Wilson-Dirac operator violating chiral symmetry at the scale of the cutoff [1,2], reflects among others in the fact that the quark masses are not protected from additive renormalizations and that the leading lattice effects in physical matrix elements and amplitudes are proportional to the lattice spacing a rather than being of $O(a^2)$.

Nowadays, a systematic approach based on the Symanzik improvement programme [3,4] is well established to permit a removal of these discretization errors of $O(a)$ in lattice QCD with confidence. It has been elaborated for on-shell quantities in refs. [5,6] and adds appropriate higher-dimensional operators to the action and fields in order to compensate for any correction terms at $O(a)$.

Within this framework a mostly non-perturbative $O(a)$ improvement of the action and the quark currents as well as their renormalization has been achieved in the quenched case, where quark loops are ignored. The basic idea for the practical implementation of on-shell improvement to enable a numerical computation of these improvement coefficients — pioneered by the ALPHA collaboration — is to exploit chiral symmetry restoration and certain chiral Ward identities from Euclidean current algebra relations on the lattice at $O(a)$ [7,8]. Most prominently, demanding the PCAC relation $\partial_\mu A_\mu^a = 2mP^a$ between the isovector axial current A_μ^a and pseudoscalar density P^a to hold as a renormalized operator identity, imposes a sensible improvement condition in this respect. As a result, the values of the improvement coefficients c_{sw} , c_A and c_V , which are required to completely eliminate the corresponding $O(a)$ effects, are known for $\beta = 6/g_0^2 \geq 6.0$, g_0 being the bare gauge coupling [9,10,11].

Therefore, one is now interested in the quality of scaling behaviour and the size of its possible violation. During the last two years it was reported in this context [12,13,14] that at $a \simeq 0.1$ fm the residual $O(a^2)$ lattice artifacts may be still fairly large e.g. for the kaon decay constant f_{Kr_0} (~ 10 %), while they are very small already for other quantities like the rho meson mass $m_\rho/\sqrt{\sigma}$ (~ 2 %) [14,15]. Thus, restricting to an intermediate physical volume, the present scaling tests are intended to examine the impact of full $O(a)$ improvement in quenched lattice QCD thoroughly and with high accuracy for different observables. Some of these are designed to coincide with phenomenologically relevant observables in the limit of large physical volumes. A preliminary status of this work has been briefly surveyed recently in ref. [16].

We wish to point out that the present investigation must be distinguished from similar studies like [13,17,18] for an important reason. Namely, since we address directly the scaling behaviour of correlation functions in finite volume, we do not have to rely on the asymptotic behaviour of (ratios of) usual timeslice correlation functions to extract, for instance, hadron masses or decay constants; these more conventional techniques often reveal to be genuinely affected by systematic errors difficult to control. Actually, an avoidance of such intrinsic uncertainties is supplied in part by the Schrödinger functional: its finite-volume fermionic correlation functions are scaling quantities at any fixed

distance in time, if the renormalization factors of the quark fields at the boundaries are properly divided out. Beyond that, they decay very slowly for small time separations, allow to gain a good numerical precision and hence offer the appealing possibility to probe the theory for $O(a)$ improvement without unwanted additional sources of errors. Finally, for sufficiently large volumes the correlators can be shown to embody standard hadronic masses and matrix elements [19]. These aspects provide the real advantages of our method. The prize to pay for it is, however, that within the Schrödinger functional formulation there exist two further improvement coefficients multiplying the boundary counterterms. These are perturbatively known only and as a consequence, one can in principle not exclude that the theory is to some extent still contaminated with uncancelled $O(a)$ contributions. That this fear can be dismissed in practice has recently been demonstrated for the renormalization group invariant running quark mass [20], but we will make sure of it in the present context too.

The paper is organized as follows. In section 2 we introduce the fermionic correlation functions under study and sketch how spectral observables can be constructed from them in the Schrödinger functional scheme. After a short account on the numerical simulations, section 3 contains a detailed description of the scaling test and the careful evaluation of the data. Section 4 gives the results. Here, also the question will be answered whether an improvement condition, chosen to fix a certain improvement coefficient non-perturbatively, is unambiguous in the sense that it automatically implies appreciably small scaling violations of $O(a^2)$ in other quantities not related to this specific condition. We conclude with a discussion in section 5.

2 Correlation functions and hadronic observables

The basic framework for our lattice setup is the QCD Schrödinger functional (SF), whose concepts and characteristic features have been published in much detail in refs. [21,22,23]; consult also [24,25] for comprehensive overviews on the subject.

It is defined as the partition function of QCD in a cylindrically shaped space-time manifold of extension $L^3 \times T$ with periodic boundary conditions in the space directions and (in general inhomogeneous) Dirichlet boundary conditions at times $x_0 = 0$ and $x_0 = T$. This means in the case of the gluons to require the spatial gauge field components at the boundaries to satisfy $A_k(x)|_{x_0=0} = C_k(\mathbf{x})$ and $A_k(x)|_{x_0=T} = C'_k(\mathbf{x})$, where C_k and C'_k are some prescribed smooth classical (chromo-electric) gauge potentials, and a similar assignment is imposed on the quark fields as well. One of the bold advantages of such a choice is that it ensures frequency gaps for the gluon and quark fields, and thereby numerical simulations at vanishing quark masses become tractable. As in most of the other applications of the QCD SF, we assume the special choice of homogeneous boundary conditions from now on: $C_k = C'_k = 0$ for the spatial components of the gauge potentials and vanishing fermion boundary fields.

2.1 Correlation functions in the Schrödinger functional

Although the definitions of fermionic correlation functions within the SF already appeared in the literature [7,9,10,11], let us recall them here and collect the essential properties and formulae in order to make the paper self-contained.

If ζ and $\bar{\zeta}$ denote ‘boundary quark and antiquark fields’ at Euclidean time $x_0 = 0$ and primed symbols the corresponding objects at $x_0 = T$ [7], one builds up the boundary field products

$$\mathcal{O}^a = a^6 \sum_{\mathbf{y}, \mathbf{z}} \bar{\zeta}(\mathbf{y}) \gamma_5 \frac{1}{2} \tau^a \zeta(\mathbf{z}), \quad \mathcal{O}'^a = a^6 \sum_{\mathbf{u}, \mathbf{v}} \bar{\zeta}'(\mathbf{u}) \gamma_5 \frac{1}{2} \tau^a \zeta'(\mathbf{v}) \quad (2.1)$$

and analogously,

$$\mathcal{Q}_k^a = a^6 \sum_{\mathbf{y}, \mathbf{z}} \bar{\zeta}(\mathbf{y}) \gamma_k \frac{1}{2} \tau^a \zeta(\mathbf{z}), \quad \mathcal{Q}'_k{}^a = a^6 \sum_{\mathbf{u}, \mathbf{v}} \bar{\zeta}'(\mathbf{u}) \gamma_k \frac{1}{2} \tau^a \zeta'(\mathbf{v}), \quad (2.2)$$

where τ^a , $a = 1, 2, 3$, are the Pauli-matrices acting on the first two flavour components of the quark fields ψ . In the operator language of quantum field theory they create initial and final quark-antiquark states with zero momenta, respectively, and transform according to the vector representation of the exact isospin symmetry. For the axial-vector current A_μ^a and the pseudoscalar density P^a we use the local expressions

$$A_\mu^a(x) = \bar{\psi}(x) \gamma_\mu \gamma_5 \frac{1}{2} \tau^a \psi(x), \quad P^a(x) = \bar{\psi}(x) \gamma_5 \frac{1}{2} \tau^a \psi(x), \quad (2.3)$$

while the vector current V_μ^a and the anti-symmetric tensor field $T_{\mu\nu}^a$ read

$$V_\mu^a(x) = \bar{\psi}(x) \gamma_\mu \frac{1}{2} \tau^a \psi(x), \quad T_{\mu\nu}^a(x) = i \bar{\psi}(x) \sigma_{\mu\nu} \frac{1}{2} \tau^a \psi(x). \quad (2.4)$$

Now we consider correlation functions on the lattice in the SF. By inserting the preceding densities at some inner point x of the SF cylinder (with support on the hypersurface at x_0) between the appropriate external quark-antiquark states, one introduces the expectation values

$$f_A(x_0) = -a^6 \sum_{\mathbf{y}, \mathbf{z}} \frac{1}{3} \langle A_0^a(x) \bar{\zeta}(\mathbf{y}) \gamma_5 \frac{1}{2} \tau^a \zeta(\mathbf{z}) \rangle = -\frac{1}{3} \langle A_0^a(x) \mathcal{O}^a \rangle \quad (2.5)$$

$$f_P(x_0) = -a^6 \sum_{\mathbf{y}, \mathbf{z}} \frac{1}{3} \langle P^a(x) \bar{\zeta}(\mathbf{y}) \gamma_5 \frac{1}{2} \tau^a \zeta(\mathbf{z}) \rangle = -\frac{1}{3} \langle P^a(x) \mathcal{O}^a \rangle, \quad (2.6)$$

analogously,

$$k_V(x_0) = -\frac{1}{9} \langle V_k^a(x) \mathcal{Q}_k^a \rangle \quad (2.7)$$

$$k_T(x_0) = -\frac{1}{9} \langle T_{k0}^a(x) \mathcal{Q}_k^a \rangle, \quad (2.8)$$

and the boundary-boundary correlation function

$$f_1 = -\frac{1}{3L^6} \langle \mathcal{O}'^a \mathcal{O}^a \rangle. \quad (2.9)$$

Gauge invariant correlators of this type have already been used to study the conservation of currents on the lattice and to deduce suitable improvement and normalization conditions in lattice QCD in order to calculate the corresponding coefficients and constants non-perturbatively by numerical simulations [9,10,11]. One of them, f_1 , will be utilized later to cancel the multiplicative renormalization of the boundary quark fields $\zeta, \dots, \bar{\zeta}'$. Besides on the SF characteristic kinematical variables [7], the correlation functions depend on the bare parameters g_0 , m_0 and the improvement coefficient $c_{\text{sw}} = c_{\text{sw}}(g_0)$ in the fermionic part of the lattice action, but not on the spatial coordinates of x owing to translation invariance. There is also a dependence on the improvement coefficients c_t and \tilde{c}_t , which account for specific boundary $O(a)$ counterterms arising in the SF approach [7].

After contracting the quark fields, all the bare and unimproved correlation functions have the general structure $h_X(x_0) \propto \langle \text{Tr} \{ H^+(x) \Gamma_X H(x) \} \rangle$, $h = f, k$, where the respective insertions are $\Gamma_X \in \{-\gamma_0, 1, \gamma_k, -\sigma_{k0}\}$, $X=A, P, V, T$; the trace extends over colour, Dirac and (in principle as well) flavour indices, and the matrix H is the quark propagator from the boundary at $x_0 = 0$ to the point x in the interior of the space-time volume [9]. In the quenched approximation the expectation values are understood to be taken as path integral averages in the pure gauge theory.

We should mention that also the primed correlation functions h'_X , which are connected to h_X through a time reflection and vice versa, become relevant. Those are in the case of eqs. (2.5) and (2.6)

$$f'_A(T - x_0) = +\frac{1}{3} \langle A_0^a(x) \mathcal{O}'^a \rangle, \quad f'_P(T - x_0) = -\frac{1}{3} \langle P^a(x) \mathcal{O}'^a \rangle, \quad (2.10)$$

and similar relations apply to k_V, k'_V and k_T, k'_T . Obviously, in h'_X the currents and densities are probed by the boundary quark fields at $x_0 = T$ instead, and the argument $T - x_0$ indicates that they fall off with this distance. For vanishing gauge fields C and C' at the boundaries, our correlation functions possess the useful time reflection invariance $h_X(x_0) = h'_X(x_0)$. This allows to sum them up accordingly, and averaging over the spatial components helps to reduce the statistical noise in the Monte Carlo simulation further.

On-shell improvement at $O(a)$ for the axial and vector currents is achieved by adding the derivatives of the pseudoscalar density and the tensor current as the suitable $O(a)$ counterterms,

$$(A_I)_\mu^a(x) \equiv A_\mu^a(x) + ac_A \tilde{\partial}_\mu P^a(x) \quad (2.11)$$

$$(V_I)_\mu^a(x) \equiv V_\mu^a(x) + ac_V \tilde{\partial}_\nu T_{\mu\nu}^a(x), \quad (2.12)$$

where the improvement coefficients c_A and c_V are determined by the demand to cancel the $O(a)$ errors in lattice Ward identities, emerging from a mixing with higher-dimensional operators with the same quantum numbers [10,11]. Then the corresponding improved fermionic correlation functions are given by:

$$f_A^I(x_0) = f_A(x_0) + ac_A \tilde{\partial}_0 f_P(x_0) \quad (2.13)$$

$$k_V^I(x_0) = k_V(x_0) + ac_V \tilde{\partial}_0 k_T(x_0). \quad (2.14)$$

The lattice derivative $\tilde{\partial}_\mu \equiv \frac{1}{2}(\partial_\mu + \partial_\mu^*)$ is the symmetrized combination of the usual forward and backward difference operators ∂_μ and ∂_μ^* , acting as

$$\partial_\mu f(x) = \frac{f(x + a\hat{\mu}) - f(x)}{a}, \quad \partial_\mu^* f(x) = \frac{f(x) - f(x - a\hat{\mu})}{a}.$$

Herewith we are already in the position to write down the unrenormalized PCAC quark mass as a function of the timeslice location $a \leq x_0 \leq T - a$:

$$m(x_0) = \frac{\tilde{\partial}_0 f_A(x_0) + ac_A \partial_0^* \partial_0 f_P(x_0)}{2f_P(x_0)}. \quad (2.15)$$

For the properly chosen value of $c_A = c_A(g_0)$ at given gauge coupling g_0 and any hopping parameter κ it is defined by obeying the PCAC relation (for two degenerate quark flavours) up to cutoff effects of $O(a^2)$,

$$\tilde{\partial}_\mu [(A_I)_\mu^a(x)] = 2mP^a(x) + O(a^2), \quad (2.16)$$

which more rigorously must be looked at as a renormalized operator identity

$$\tilde{\partial}_\mu \langle (A_R)_\mu^a(x) \mathcal{O} \rangle = 2m_R \langle P_R^a(x) \mathcal{O} \rangle + O(a^2)$$

in terms of some arbitrary renormalized on-shell $O(a)$ improved field \mathcal{O} localized in a region not containing x .

2.2 Construction of renormalized observables

Now we want to introduce the renormalized correlation functions and design the scaling combinations of them, which will be studied numerically in the next section.

The QCD SF serves as a particular intermediate finite-volume renormalization scheme which is, however, not necessarily related to a special regularization [7,24,25]. Here, the SF is employed as a mass-independent renormalization scheme, while the ratio T/L is assumed to be kept fixed to a certain value. The freedom in choosing the boundary fields C and C' (as well as the boundary conditions on the quark fields specified by angles θ_μ , cf. subsection 3.1) different from zero are left for other applications, see e.g. [9,20,26]. Moreover, the SF respects $O(a)$ improvement after adding the $O(a)$ counterterms $\propto c_t, \tilde{c}_t$ so that by attaching additive and multiplicative renormalization constants, the quantities

$$(A_R)_\mu^a(x) = Z_A(1 + b_A am_q)(A_I)_\mu^a(x) \quad (2.17)$$

$$(V_R)_\mu^a(x) = Z_V(1 + b_V am_q)(V_I)_\mu^a(x) \quad (2.18)$$

$$P_R^a(x) = Z_P(1 + b_P am_q)P^a(x) \quad (2.19)$$

induce the renormalized and improved correlation functions

$$f_A^R(x_0) = Z_A(1 + b_A am_q) Z_\zeta^2 (1 + b_\zeta am_q)^2 f_A^I(x_0) \quad (2.20)$$

$$k_V^R(x_0) = Z_V(1 + b_V am_q) Z_\zeta^2 (1 + b_\zeta am_q)^2 k_V^I(x_0) \quad (2.21)$$

$$f_P^R(x_0) = Z_P(1 + b_P am_q) Z_\zeta^2 (1 + b_\zeta am_q)^2 f_P^I(x_0) \quad (2.22)$$

$$f_1^R = Z_\zeta^4 (1 + b_\zeta am_q)^4 f_1. \quad (2.23)$$

The constants Z_ζ and b_ζ (the former being scale dependent [7]) have to be attributed to the boundary values of the quark and antiquark fields appearing in the products (2.1) and (2.2) in the renormalized theory. In a mass-independent renormalization scheme the underlying $O(a)$ counterterm enters as

$$\zeta_R(\mathbf{x}) = Z_\zeta(1 + b_\zeta am_q) \zeta(\mathbf{x})$$

and similarly for the antiquark field $\bar{\zeta}$, giving $\mathcal{O}_R^a = Z_\zeta^2(1 + b_\zeta am_q)^2 \mathcal{O}^a$ for instance.

Because the renormalization does not distinguish between different flavours in a mass-independent scheme, the knowledge of the Z -factors suffices to link the lattice theory at finite cutoff to the renormalized continuum theory. Here, all normalization conditions to fix and determine the renormalization constants Z_X and b_X , $X=A,V,P$, were imposed on appropriate matrix elements at *zero quark mass*, which is safe within the SF scheme as the finite lattice extent L provides the before-mentioned natural infrared cutoff for the theory [9,10]. Because of the zero quark mass condition they are functions of g_0 only and *not* of the subtracted bare quark mass, which equals

$$am_q = am_0 - am_c(g_0) = \frac{1}{2} \left(\frac{1}{\kappa} - \frac{1}{\kappa_c} \right) \quad (2.24)$$

and vanishes along a critical line $m_0 = m_c(g_0)$ in the plane of bare parameters, implicitly defining the critical hopping parameter κ_c . Any remaining corrections of $O(am_q)$ are supposed to be cancelled by adjusting the b_X alone.

Now we can pass to the set of observables we have constructed for the present study. We start with the renormalized PCAC (current) quark mass in the SF scheme, which in view of eqs. (2.15), (2.17) and (2.19) may be defined as

$$\bar{m} = \frac{Z_A}{Z_P(L)} m \left(\frac{T}{2} \right) \quad (2.25)$$

by multiplying the proper renormalization constants Z_A and $Z_P(L)$, the latter assumed to be taken at some renormalization scale $\mu = 1/L$ [20,27]. Strictly speaking, the ratio of the additive renormalization factors $1 + b_A am_q$ and $1 + b_P am_q$ would have been to be accounted for as well, but it turns out perturbatively [28] and non-perturbatively [29] that $(b_A - b_P) am_q$ is numerically quite small at the interesting values of the bare gauge coupling and the hopping parameter. Hence we neglect it, here.

Beyond that, we compose the following (time dependent) combinations of renormalized and improved fermionic correlation functions. Firstly, the logarithmic time derivatives

$$\mu_{\text{PS}}(x_0) = \frac{\tilde{\partial}_0 f_{\text{P}}^{\text{R}}(x_0)}{f_{\text{P}}^{\text{R}}(x_0)} = \frac{\tilde{\partial}_0 f_{\text{P}}(x_0)}{f_{\text{P}}(x_0)} \quad (2.26)$$

$$\mu_{\text{V}}(x_0) = \frac{\tilde{\partial}_0 k_{\text{V}}^{\text{R}}(x_0)}{k_{\text{V}}^{\text{R}}(x_0)} = \frac{\tilde{\partial}_0 k_{\text{V}}^{\text{I}}(x_0)}{k_{\text{V}}^{\text{I}}(x_0)} \quad (2.27)$$

of the respective SF correlation functions in the pseudoscalar and vector meson channel; they deviate from the ordinary definition of effective masses ($\sim \partial_0 \ln h_{\text{X}}$) by terms of $\mathcal{O}(a^2)$. Secondly, we will consider the ratios

$$\begin{aligned} \eta_{\text{PS}}(x_0) &= C_{\text{PS}} \frac{f_{\text{A}}^{\text{R}}(x_0)}{\sqrt{f_1^{\text{R}}}} \\ &= C_{\text{PS}} \frac{Z_{\text{A}}(1 + b_{\text{A}}am_{\text{q}})f_{\text{A}}^{\text{I}}(x_0)}{\sqrt{f_1}}, \quad C_{\text{PS}} = \frac{2}{\sqrt{L^3 \mu_{\text{PS}}(\frac{T}{2})}} \end{aligned} \quad (2.28)$$

$$\begin{aligned} \eta_{\text{V}}(x_0) &= C_{\text{V}} \frac{k_{\text{V}}^{\text{R}}(x_0)}{\sqrt{f_1^{\text{R}}}} \\ &= C_{\text{V}} \frac{Z_{\text{V}}(1 + b_{\text{V}}am_{\text{q}})k_{\text{V}}^{\text{I}}(x_0)}{\sqrt{f_1}}, \quad C_{\text{V}} = \frac{2}{\sqrt{L^3 [\mu_{\text{V}}(\frac{T}{2})]^3}}. \end{aligned} \quad (2.29)$$

Since through the division by $\sqrt{f_1^{\text{R}}}$ the renormalization factors of the boundary quark fields, $Z_{\zeta}(1 + b_{\zeta}am_{\text{q}})$, drop out, it is ensured that η_{PS} and η_{V} (at fixed argument x_0) exhibit scaling and have a well-defined continuum limit. We note in passing that alternatively the correlation function f_{A}^{I} also could have been used instead of f_{P} to define a ‘local mass’ in the pseudoscalar channel. But as f_{A}^{I} amounts to somewhat larger statistical errors in the time derivatives, we here preferred f_{P} for the purpose of $\mu_{\text{PS}}(x_0)$.

In the present scaling test we fix a definite temporal separation from the boundaries, $x_0 = T/2$. Thus one arrives at the objects

$$\text{pseudoscalar channel :} \quad \mu_{\text{PS}}\left(\frac{T}{2}\right) \quad \eta_{\text{PS}}\left(\frac{T}{2}\right) \quad (2.30)$$

$$\text{vector channel :} \quad \mu_{\text{V}}\left(\frac{T}{2}\right) \quad \eta_{\text{V}}\left(\frac{T}{2}\right). \quad (2.31)$$

Their continuum limits are expected to be approached like $\mu_{\text{X}}(\frac{T}{2}) + \mathcal{O}(a^2)$ and $\eta_{\text{X}}(\frac{T}{2}) + \mathcal{O}(a^2)$, $\text{X}=\text{PS},\text{V}$, in the $\mathcal{O}(a)$ improved theory. The choice $x_0 = T/2$ is motivated by the fact that in the SF scheme cutoff effects are generically larger when sitting closer to the boundaries. It is possible to construct other quantities in a similar way, but we consider the foregoing ones as reasonably representative.

Let us emphasize, however, a final point. Adopting the quantum mechanical representation of the field operators associated to (2.3) and (2.4), it can be shown in the transfer matrix formalism that asymptotically for large Euclidean times the quantities in eqs. (2.30) and (2.31) become the pseudoscalar and vector meson masses ($\mu_{\text{PS}}, \mu_{\text{V}}$) as well as the pseudoscalar decay constant (η_{PS}). For instance, the proportionality constant C_{PS} in (2.28) is such that this ratio turns, as the temporal lattice extent goes to infinity ($x_0, T - x_0 \rightarrow \infty$), into a familiar matrix element, which complies with the standard definition of the pion decay constants in continuum QCD:

$$Z_{\text{A}} \langle 0 | \bar{\psi}(x) \gamma_0 \gamma_5 \frac{1}{2} \tau^a \psi(x) | \pi^a(\mathbf{0}) \rangle = m_{\pi} f_{\pi}.$$

More formally, the observables \mathcal{O} just introduced should be regarded as functions $\mathcal{O}(T/L, x_0/L, L/r_0, a/r_0)$, and in the spirit of the above a physically meaningful situation is realized if, as the spatial volume $(L/a)^3$ tends to infinity, $x_0 \gg r_0$ and $T - x_0 \gg r_0$ are valid for some typical hadronic radius of $r_0 \simeq 0.5$ fm. Masses and matrix elements of interest in hadron phenomenology can then be extracted [19].

3 Scaling tests

Before going into the details of the investigation, one has to keep in mind that here the actually taken lattice volumes in physical units are only of intermediate magnitude. Therefore, any of the following results are prevented from resembling the large volume limit, where our observables were argued to receive a really physical meaning. Instead of this, most emphasis is on the scaling properties of the theory, which should not depend on the specific choice of the lattice size and the SF characteristic boundary conditions. Nevertheless, we refer from now on to the (first three of the) quantities in eqs. (2.30) and (2.31) as the ‘pion mass’, its decay constant and the ‘rho meson mass’ and assign the common symbols m_{π} , f_{π} and m_{ρ} to them in the obvious manner. We also denote $\bar{\eta}_{\text{V}} \equiv \eta_{\text{V}}(\frac{T}{2})$ in the vector meson channel.

The advantage of working at finite quark mass in a direct test of improvement should be stressed explicitly. Namely, this avoids any extrapolations and evades the potential problems with so-called exceptional configurations one runs into, when the parameter region of zero quark mass is attempted to be reached [9,30].

3.1 Monte Carlo simulation

The cost of a quenched QCD simulation is always governed by the computation of fermion propagators required for the correlation functions to be covered. This involves the action of the Wilson-Dirac operator on quark fields $\psi(x)$, which for the $\mathcal{O}(a)$ improved theory in the framework of the SF is conveniently decomposed as $D + \delta D + m_0$ with

$$(D + m_0)\psi(x) \equiv \frac{1}{2\kappa} M\psi(x), \quad \kappa = \frac{1}{8 + 2m_0} \quad (3.1)$$

$$\begin{aligned}
M\psi(x) = \psi(x) - \kappa \sum_{\mu=0}^3 \left\{ \lambda_\mu U(x, \mu) (1 - \gamma_\mu) \psi(x + a\hat{\mu}) \right. \\
\left. + \lambda_\mu^* U(x - a\hat{\mu}, \mu) (1 + \gamma_\mu) \psi(x - a\hat{\mu}) \right\}, \quad (3.2)
\end{aligned}$$

where, as usual, the fermionic degrees of freedom $\psi(x)$ live on the sites x of the lattice, and $U(x, \mu)$ denotes the $SU(3)$ -valued gauge links in lattice direction $x + a\hat{\mu}$, $\mu = 0, \dots, 3$. The factors $\lambda_\mu = e^{ia\theta_\mu/L}$, $\theta_0 \equiv 0$, give rise to a modified covariant derivative equivalent to demanding spatial periodicity of the quark field up to a phase $e^{i\theta_k}$; for our purposes θ_k , $k = 1, 2, 3$, was set to zero throughout.¹ The local $O(a)$ counterterm $\delta D = \delta D_v + \delta D_b$ now consists of two contributions, namely the Sheikholeslami-Wohlert clover term [31]

$$\delta D_v \psi(x) = c_{sw} \frac{i}{4} a \sigma_{\mu\nu} F_{\mu\nu}(x) \psi(x) \quad (3.3)$$

and a term

$$\begin{aligned}
\delta D_b \psi(x) = (\tilde{c}_t - 1) \left\{ \delta_{x_0/a, 1} [\psi(x) - U(x - a\hat{0}, 0)^+ P_+ \psi(x - a\hat{0})] \right. \\
\left. + \delta_{x_0/a, T-1} [\psi(x) - U(x, 0) P_- \psi(x + a\hat{0})] \right\} \quad (3.4)
\end{aligned}$$

with

$$P_+ \psi(x) \Big|_{x_0=0} = 0, \quad P_- \psi(x) \Big|_{x_0=T} = 0, \quad P_\pm \equiv \frac{1}{2} (1 \pm \gamma_0),$$

which is specific for the SF type of boundary conditions in our setup. The improvement coefficient \tilde{c}_t and a further one, c_t which enters the calculation as well but is independent of the local composite operators containing quark fields and thus not written down here, are set to their one-loop perturbative values.²

Since the technicalities of the Monte Carlo simulations are identical to those already detailed in ref. [9], it is not necessary to repeat them here in full length. Our data were taken on the APE-100 massively parallel computers with 128 – 512 nodes at DESY Zeuthen, whose topology also allows to simulate independent replica of the system at the same time in the case of smaller lattice volumes (sets A – C below). The gauge field ensembles were generated by a standard hybrid overrelaxation algorithm, where each iteration consists of one heatbath step followed by several microcanonical reflection steps (typically $N_{OR} = L/2a + 1$), and the correlation functions have been evaluated by averaging over sequential gauge field configurations separated by 50 iterations. To solve the system of linear equations belonging to the boundary value problem of the Dirac operator within the measurements of the correlators, the BiCGStab algorithm with even-odd preconditioning was used as inverter. Finally, a single-elimination jackknife procedure was applied to estimate the statistical errors of all the secondary quantities,

¹ In general, θ_k can serve as an additional kinematical variable to formulate proper improvement and normalization conditions, see for instance [9,20].

² Recently, the coefficient c_t has also been computed up to two-loop order of perturbation theory in the quenched case [32].

because the data stemming from the same configurations must be considered as strongly correlated. By dividing the full ensemble of measurements into bins we also checked for the statistical independence of our data samples.

3.2 Method and numerical analysis

For the analysis we use c_{sw} , c_X , Z_X , $X=A,V,P$, and b_V non-perturbatively determined in [9,10,11,20] for $\beta \geq 6.0$, while b_A and b_P are taken from one-loop perturbation theory [7,8,28]. If available, we always adopted the rational formulas for the former with overall, i.e. statistical and systematic, uncertainties stated in the references. As opposed to Z_A and Z_V (and as already anticipated below eq. (2.25) in subsection 2.2), the normalization constant of the pseudoscalar density, $Z_P = Z_P(L)$, acquires a scale dependence through its renormalization. The scale evolution of Z_P , which due to its definition at the point of vanishing PCAC quark mass (but in the absence of exact chiral symmetry at finite a) is unique only up to $O(a^2)$ errors, has been recently computed non-perturbatively in [20]. In the SF the appropriate renormalization scale is $\mu = 1/L \equiv 1/2L_{\text{max}}$, with $L_{\text{max}}/r_0 = 0.718$ [33], and we take over the needed numbers for Z_P from the last but one reference. In the case of c_V and the critical hopping parameter κ_c in eq. (2.24), where no closed expressions are recommended yet, we adapted the numbers at discrete values of the gauge coupling from refs. [9,11] to our simulated β -values by linear interpolation.

The strategy was then to keep a finite physical volume and the quark mass fixed by prescribing the geometry $T/L = 2$ and two further renormalization conditions, which we decided to chose as

$$m_\pi L = 2.0 \quad \text{and} \quad \frac{L}{r_0} = 1.49 \quad (3.5)$$

for the ‘pseudoscalar meson (pion) mass’ and the spatial lattice size, respectively. The first condition on m_π can be, at least approximately³, satisfied by a careful tuning of the hopping parameter ($a^2 m_\pi^2 \sim \kappa$). Here the reference scale is expressed by the hadronic radius r_0 defined in [34] through the force between static quarks to yield the phenomenologically motivated value of $r_0 \simeq 0.5$ fm. Using the latest results on the hadronic scale r_0/a in ref. [33], quoted there as

$$\ln\left(\frac{a}{r_0}\right) = -1.6805 - 1.7139(\beta - 6) + 0.8155(\beta - 6)^2 - 0.6667(\beta - 6)^3, \quad (3.6)$$

one can solve numerically for β after inserting $a/r_0 = 1.49a/L$ to find the desired pairs $(L/a, \beta)$ in order to fulfill the second condition in eq. (3.5) within errors. In practice, the particular value $L/r_0 = 1.49$ was determined by the initial simulations at $\beta = 6.0$ on lattices with spatial size $L/a = 8$, and the larger lattices were adjusted thereafter. The simulation parameters and some results are compiled in table 1. These settings give an intermediate volume of $(0.75^3 \times 1.5)$ fm⁴, and one moves on a line of constant

³ In our actual simulations we have some mismatch in $m_\pi L$ between the individual points in parameter space, which will be discussed later.

set	L/a	β	κ	N_{meas}	L/r_0	am_π	$m_\pi L$
A	8	6.0	0.13458	12800	1.490(6)	0.2505(11)	2.004(9)
B	10	6.14	0.13538	3840	1.486(7)	0.1945(14)	1.946(14)
C	12	6.26	0.13546	2560	1.495(7)	0.1709(13)	2.050(16)
D	16	6.48	0.13541	3000	1.468(8)	0.1244(9)	1.991(15)

Table 1: Simulation points and its statistics N_{meas} denoting the number of gauge field configurations, on which the fermionic correlation functions were computed. L/r_0 and $m_\pi L$ are the quantities chosen to fix renormalization conditions for the LCP studied.

physics (LCP) in bare lattice parameter space with lattice resolutions ranging from 0.1 fm to 0.05 fm.

As an important prerequisite for the reliability of the scaling test we had, of course, to estimate the dependence of our results on the SF specific (and solely perturbatively known) improvement coefficients of the boundary counterterms c_t and \tilde{c}_t , which with respect to full non-perturbative $O(a)$ improvement represent the only imperfectly known input parameters for the simulation. Otherwise a complete suppression of errors linear in a would not be guaranteed, and continuum limit extrapolations with an $O(a^2)$ term as the dominant scaling violation is a priori not justified. To this end we verified by an artificial variation of the one-loop coefficients in the expansions [26,35]

$$c_t^{1\text{-loop}} = 1 - 0.089g_0^2 + O(g_0^4) \quad (3.7)$$

$$\tilde{c}_t^{1\text{-loop}} = 1 - 0.018g_0^2 + O(g_0^4) \quad (3.8)$$

by a factor 2 for $c_t^{1\text{-loop}}$ and by a factor 10 for $\tilde{c}_t^{1\text{-loop}}$ that at unchanged renormalization conditions (3.5) their influence on the level of numerical precision in our data is small enough to be neglected: it typically came out to be below 1 % for af_π , below 2 % for $\bar{\eta}_V$, and nearly not visible for am and am_ρ , at parameters corresponding to simulation point A ($T/a = 16$). It was sufficient to do these replacements for the lattice with the largest a , since the relative contribution of the boundaries to the field variables residing on the bulk of lattice points among a given gauge field configuration decreases with decreasing lattice spacing. Therefore, the leading scaling violations can be regarded as being purely $O(a^2)$ within our precision.

In figure 1 we first illustrate for simulation points A and D the correlation functions f_A , f_P and some of the quantities deduced from them in the previous section in dependence of the time coordinate. The correlators reflect that a good signal remains also at larger distances in time. The PCAC quark mass (2.15) already exposes a plateau for the rather moderate temporal extensions of the lattice, whereas the ‘local pion mass’ (2.26), and even more the logarithmic derivative of the improved correlation of the axial current (2.13), show significant contributions from higher intermediate states in small volumes. On physically large volumes, however, this pattern disappears: plateaux develop around $x_0 = T/2$, i.e. the lightest excitations, which coincide with the pseudoscalar meson mass

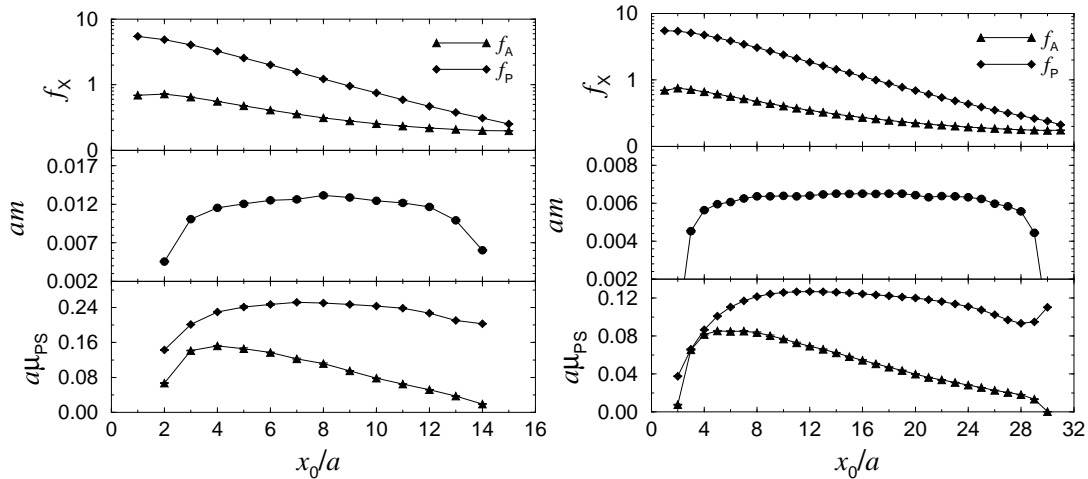


Figure 1: Correlation functions f_A and f_P (upper parts) and $O(a)$ improved local masses extracted from them: PCAC current quark mass via eq. (2.15) (middle part) and ‘pseudoscalar meson masses’ via eq. (2.26) and the same with f_P substituted by f_A^I (lower parts). The left figure depicts simulation point A ($L/a = 8$) and the right one point D ($L/a = 16$), with $T/L = 2$ in both cases. The solid lines are only meant to guide the eye, and the statistical errors are smaller than the symbols.

when defined either by f_A^I or by f_P , govern the exponential decay of these functions. This will be explicitly demonstrated elsewhere [19]. An analogous statement holds for the vector meson mass via the correlation functions k_V^I and k_T .

The expectation values in the simulation points of table 1 for the observables eqs. (2.15), (2.30) and (2.31) are now summarized in table 2. Within all potential sources of errors to be incorporated in the analysis, i.e. the statistical one and those coming from Z_A/Z_P , Z_A , Z_V , L/r_0 and $m_\pi L$, the contributions caused by the uncertainties of the renormalization factors Z_X ever dominate the combined errors quoted in the second parentheses in the table. Furthermore, any inherent small mismatch of the central values with the renormalization conditions (3.5) on $m_\pi L$ and L/r_0 in sets B, C and D was corrected by a conservative estimation of the slopes $\partial\mathcal{O}/\partial(am_\pi)$ and $\partial\mathcal{O}/\partial\beta$ with $\mathcal{O} = \mathcal{O}(m_\pi L, L/r_0, L/a) \in \{am, am_\rho, af_\pi, \bar{\eta}_V\}$, which enter the identities for the required partial derivatives

$$\frac{\partial\mathcal{O}}{\partial(m_\pi L)} \simeq \frac{a}{L} \frac{\partial\mathcal{O}}{\partial(am_\pi)} \quad (3.9)$$

$$\frac{\partial\mathcal{O}}{\partial(L/r_0)} \simeq \frac{a}{L} \frac{\partial\beta}{\partial(a/r_0)} \frac{\partial\mathcal{O}}{\partial\beta} \simeq \frac{r_0}{a} \frac{\partial\mathcal{O}}{\partial(L/a)}. \quad (3.10)$$

They were numerically extracted in linear approximation from several simulations in set A at neighbouring values of κ and β , where in the latter case they had to be combined with the derivative $\partial\beta/\partial(a/r_0)$ to be read off from the parametrization eq. (3.6). The slopes obtained in this way were carried over to the finer lattices as well, since for

increasing lattice resolution ($\beta > 6.0$) their corrections are of $O(a)$ and, with respect to the other sources of errors, can safely be ignored.

set	$am(\frac{T}{2})$	am_ρ	af_π	$\bar{\eta}_V$
A	0.0132(2)	0.3438(10)	0.1248(5)(13)	0.3283(19)(25)
B	0.0083(1)	0.2688(15)	0.1013(7)(12)	0.3387(36)(40)
C	0.0096(1)	0.2337(14)	0.0851(7)(11)	0.3289(40)(43)
D	0.00651(6)	0.1689(10)	0.0650(5)(8)	0.3561(41)(44)

Table 2: Analysis results for the observables under consideration in lattice units. The first error is only the statistical one, the second one (where given) includes in addition the uncertainties from the renormalization constants.

4 Results

We pass to the final results. After the procedure of matching the conditions characterizing the LCP under study, one finds the numbers collected in table 3; note that according to (2.25) the bare PCAC quark mass $m(\frac{T}{2})$ translates through multiplication with Z_A/Z_P into the renormalized quantity \bar{m} . Now we are prepared to perform ex-

set	$\bar{m}r_0$	$m_\rho r_0$	$f_\pi r_0$	$\bar{\eta}_V$
A	0.1069(50)	1.846(13)	0.6701(82)	0.3283(46)
B	0.1029(35)	1.839(15)	0.684(11)	0.3296(72)
C	0.1045(36)	1.848(18)	0.681(13)	0.3360(95)
D	0.1103(35)	1.860(18)	0.699(12)	0.3457(75)

Table 3: Dimensionless results for the quantities of table 2 with total errors after they have been corrected to fulfill exactly the simultaneous renormalization conditions (3.5) as described in the text (subsection 3.2). The errors on r_0/a quoted in [33] have been taken into account as well.

trapolations of these data to the continuum limit, assuming convergence with a rate proportional to a^2 .

The fits are displayed in figures 2 – 5 and exemplify the scaling behaviour on the course from simulation points A to D. One evidently observes the leading corrections to the continuum to be compatible with $O(a^2)$. Moreover, it can be inferred from table 4 that the differences of the continuum limits from the values at $\beta = 6.0$ ($a \simeq 0.1$ fm) are around or even below 5 % in the improved theory. These appear to be partly smaller than it was to be expected on basis of the experiences reported previously in refs. [13,14].

At this point we have to add the remark that the results in the vector channel had to be revised compared to those listed in [16]. Due to some incorrect normalization of the

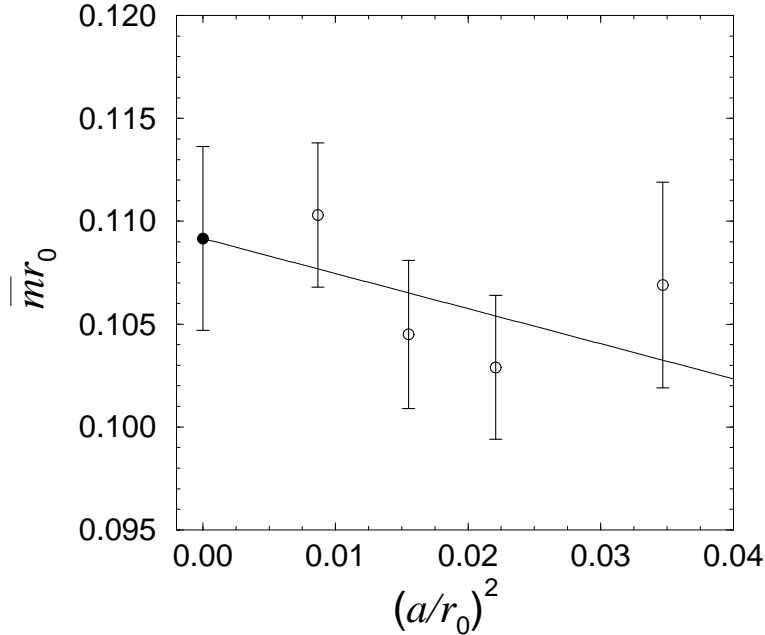


Figure 2: *Scaling behaviour of the renormalized PCAC current quark mass in units of r_0 . An intermediate volume with SF boundary conditions is considered. The renormalization constant Z_P refers to a scale of $L = 1.436 r_0$. Non-perturbative $O(a)$ improvement allows to extrapolate linearly with $(a/r_0)^2 \rightarrow 0$ to the continuum limit.*

correlation functions k_V and k_T during an earlier data analysis, we erroneously observed a quite steep slope when carrying out the $(a/r_0)^2 \rightarrow 0$ fit for the ratio $\bar{\eta}_V$ defined in eq. (2.31). Looking at the final numbers now, it does no longer stand in contradiction to the findings in the pseudoscalar channel. By contrast, since the scaling violations of $\bar{\eta}_V$ are only slightly larger than for $f_\pi r_0$, we interpret this as a further compelling and satisfactory indication for the effectiveness of non-perturbative $O(a)$ improvement.

In ref. [14] the suspicion was raised that scaling looks even slightly better, if the perturbative estimates for the improvement coefficients c_A and c_V are used. This issue deserves some comments here. In order to address the sensitivity of the analysis to the improvement terms in the pseudoscalar and vector channel proportional to c_A and c_V , we just evaluated our data with setting these coefficients arbitrarily to zero. Then, of course, the theory is only partially $O(a)$ improved, and a residual contamination with uncanceled $O(a)$ contributions has still to be expected. The surprising outcome is that upon omitting those terms, two quantities ($f_\pi r_0, \bar{\eta}_V$) have somewhat smaller a -effects in total magnitude. At the same time, however, the renormalized PCAC quark mass $\bar{m} r_0$ gets much larger ones. Nevertheless, as seen from table 4, the continuum limits of both data sets agree within errors. Such a result might suggest that the *qualitative*

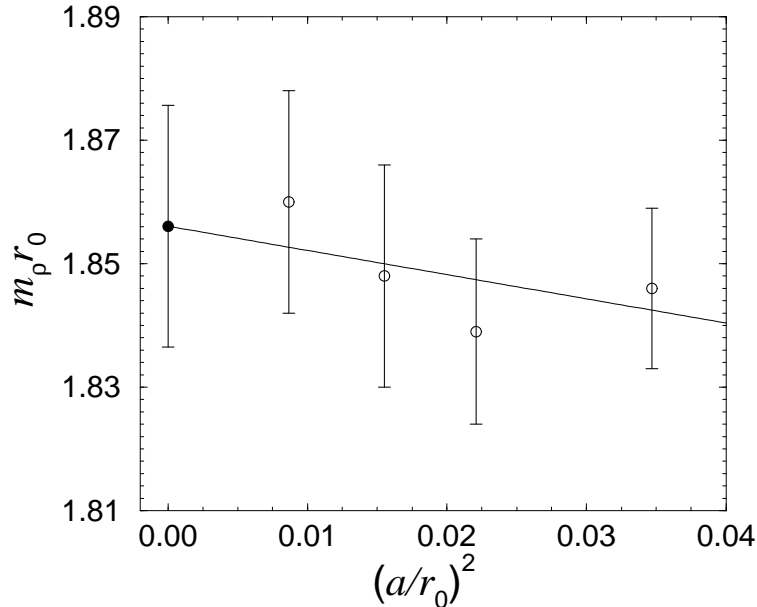


Figure 3: Continuum limit extrapolation as in figure 2 but for the ‘rho meson mass’ in intermediate volume.

scaling behaviour of our quantities (apart from $\bar{m}r_0$) is only marginally influenced by the definite choice of c_X , $X=A,V$, still meeting the condition of a dominant a^2 -behaviour. On the other hand, we observed a tendency in the $c_A = c_V = 0$ data points to disperse around the straight line fits to the continuum, which hints at some remnant of admixture of $O(a)$ discretization errors; hence a scaling violating term $\propto a^2$ in leading order rather seems to be ruled out in that case. This is particularly pronounced for $\bar{m}r_0$, where the correction to the continuum limit grows distinctly (from 2 % to 17 % in table 4) if the improvement of the axial quark current is switched off. Opposed to that, in the fully improved case including the $O(a)$ correction terms, the required continuum limit

case	$\bar{m}r_0$	$m_\rho r_0$	$f_\pi r_0$	$\bar{\eta}_V$
fully improved	0.1092(45) 2 %	1.856(20) < 1 %	0.704(13) 5 %	0.3472(84) 6 %
$c_A = 0$ and $c_V = 0$	0.1069(46) 17 %	1.856(20) < 1 %	0.698(13) 1 %	0.3439(85) 2 %

Table 4: Continuum limits and their percentage deviations from $\beta = 6.0$ ($a \simeq 0.1$ fm). The lower numbers belong to a data evaluation, where the improvement coefficients c_A and c_V have been artificially taken to vanish.

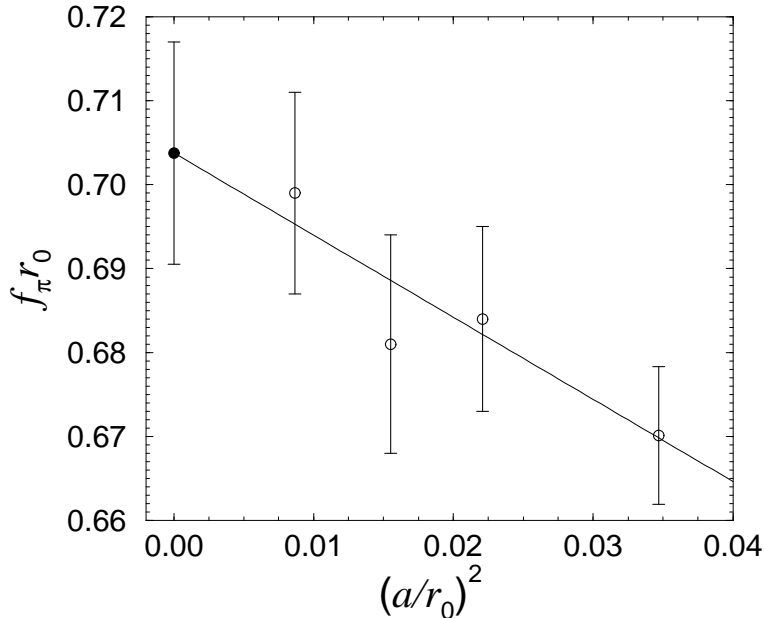


Figure 4: *The same as in figure 3 but for the ‘pion decay constant’.*

extrapolations are generically not critical. In conclusion — and as a further convincing argument for the use of its non-perturbative values — this finally supports the physical insight that c_A and c_V are essentially relevant for chiral symmetry restoration at finite cutoff.

5 Discussion and outlook

In confirmation of similar investigations [12,13,14,15], $O(a)$ improvement implies a substantial reduction of scaling violations. Our numerical simulations of renormalized correlation functions in intermediate physical volume within the Schrödinger functional give clear evidence for an overall behaviour completely consistent with being linear in a^2 at $a \leq 0.1$ fm, for all quantities under consideration. Changing a by a factor two yields very stable fits and honest continuum limit extrapolations. Actually, the residual $O(a^2)$ cutoff effects at $a \simeq 0.1$ fm stay around $(f_\pi r_0$ and $\bar{\eta}_V)$ or significantly below 5 % ($\bar{m}r_0$ and $m_\rho r_0$).

To quantify directly the influence of the improvement coefficients c_A and c_V on the scaling behaviour, we examined also the partially improved case $c_A = c_V = 0$. In this case $f_\pi r_0$ and $\bar{\eta}_V$ show an even weaker dependence on the lattice spacing, *but now one finds $\sim 17\%$ lattice spacing effects at $a \simeq 0.1$ fm* in the renormalized current quark mass $\bar{m}r_0$. Additionally, as outlined in section 4, the functional form of the leading a -effects then appears no longer compatible with a^2 alone; furthermore, chiral Ward identities

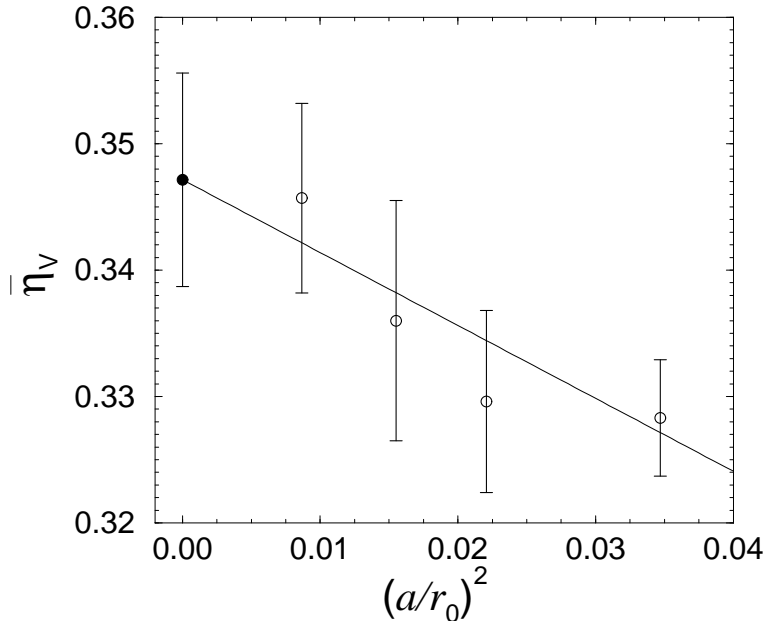


Figure 5: Again as in figure 3 but now for the observable $\bar{\eta}_V$, which is composed of a (renormalized and improved) correlation function involving the vector current.

are badly violated for $c_A = c_V = 0$ at $O(a)$ level [9,11]. Thus there is in general no choice for the improvement coefficients c_A and c_V , which diminishes the size of $O(a^2)$ lattice artifacts simultaneously for *all* relations and observables below a level of 5 %. However, one should not feel tempted to judge this fact as a kind of principal conflict with the improvement programme itself, since the criterion of small $O(a^2)$ corrections has only been touched when selecting a definite set of kinematical variables to formulate the respective improvement conditions within the Schrödinger functional.

To summarize, the scaling tests in hand illustrate that also in the $O(a)$ improved theory the remaining $O(a^2)$ discretization errors have to be assessed — and consequently can be extrapolated away reliably — by varying the lattice spacing.

An extension of the present study to physically large volumes, where hadronic masses and matrix elements can be computed, is in progress [19].

Acknowledgements

This work is part of the ALPHA collaboration research programme. We thank DESY for allocating computer time on the APE-Quadrics computers at DESY Zeuthen to this project and the staff of the computer centre at Zeuthen for their support. I am grateful to Rainer Sommer for numerous discussions, useful suggestions and a critical reading of the manuscript. I also thank Hartmut Wittig and Andreas Hoferichter for discussions.

References

- [1] M. Bochicchio, L. Maiani, G. Martinelli, G.C. Rossi and M. Testa, Nucl. Phys. B262 (1985) 331.
- [2] L. Maiani and G. Martinelli, Phys. Lett. B178 (1986) 265.
- [3] K. Symanzik, Nucl. Phys. B226 (1983) 187.
- [4] K. Symanzik, Nucl. Phys. B226 (1983) 205.
- [5] M. Lüscher and P. Weisz, Phys. Lett. 158B (1985) 250.
- [6] M. Lüscher and P. Weisz, Commun. Math. Phys. 97 (1985) 59.
- [7] ALPHA, M. Lüscher, S. Sint, R. Sommer and P. Weisz, Nucl. Phys. B478 (1996) 365, hep-lat/9605038.
- [8] R. Sommer, Nucl. Phys. Proc. Suppl. 60A (1998) 279, hep-lat/9705026.
- [9] ALPHA, M. Lüscher, S. Sint, R. Sommer, P. Weisz and U. Wolff, Nucl. Phys. B491 (1997) 323, hep-lat/9609035.
- [10] ALPHA, M. Lüscher, S. Sint, R. Sommer and H. Wittig, Nucl. Phys. B491 (1997) 344, hep-lat/9611015.
- [11] M. Guagnelli and R. Sommer, Nucl. Phys. Proc. Suppl. B63 (1998) 886, hep-lat/9709088.
- [12] QCDSF, M. Göckeler et al., Phys. Lett. B391 (1997) 388, hep-lat/9609008.
- [13] QCDSF, M. Göckeler et al., Phys. Rev. D57 (1998) 5562, hep-lat/9707021.
- [14] H. Wittig, Nucl. Phys. Proc. Suppl. B63 (1998) 47, hep-lat/9710013.
- [15] R.G. Edwards, U.M. Heller and T.R. Klassen, Phys. Rev. Lett. 80 (1998) 3448, hep-lat/9711052.
- [16] ALPHA, J. Heitger, Conference contribution to LATTICE 98, to be published in Nucl. Phys. Proc. Suppl. , hep-lat/9809002.
- [17] A. Cucchieri, M. Masetti, T. Mendes and R. Petronzio, Phys. Lett. B422 (1998) 212, hep-lat/9711040.
- [18] D. Becirevic et al., hep-lat/9809129.
- [19] ALPHA, M. Guagnelli, J. Heitger, R. Sommer and H. Wittig, in preparation.
- [20] ALPHA, S. Capitani, M. Lüscher, R. Sommer and H. Wittig, hep-lat/9810063.

- [21] M. Lüscher, R. Narayanan, P. Weisz and U. Wolff, Nucl. Phys. B384 (1992) 168, hep-lat/9207009.
- [22] S. Sint, Nucl. Phys. B421 (1994) 135, hep-lat/9312079.
- [23] S. Sint, Nucl. Phys. B451 (1995) 416, hep-lat/9504005.
- [24] R. Sommer, Non-perturbative Renormalization of QCD, Lectures given at 36th Internationale Universitätswochen für Kernphysik und Teilchenphysik, Schladming, Austria, 1 – 8 Mar 1997, hep-ph/9711243.
- [25] M. Lüscher, Advanced Lattice QCD, Lectures given at Les Houches Summer School in Theoretical Physics, Probing the Standard Model of Particle Interactions, Les Houches, France, 28 Jul – 5 Sep 1997, hep-ph/9802029.
- [26] M. Lüscher, R. Sommer, P. Weisz and U. Wolff, Nucl. Phys. B413 (1994) 481, hep-lat/9309005.
- [27] ALPHA, S. Capitani et al., Nucl. Phys. Proc. Suppl. B63 (1998) 153, hep-lat/9709125.
- [28] S. Sint and P. Weisz, Nucl. Phys. B502 (1997) 251, hep-lat/9704001.
- [29] G.M. de Divitiis and R. Petronzio, Phys. Lett. B419 (1998) 311, hep-lat/9710071.
- [30] W. Bardeen, A. Duncan, E. Eichten, G. Hockney and H. Thacker, Phys. Rev. D57 (1998) 1633, hep-lat/9705008.
- [31] B. Sheikholeslami and R. Wohlert, Nucl. Phys. B259 (1985) 572.
- [32] A. Bode and U. Wolff, Nucl. Phys. B540 (1999) 491, hep-lat/9809175.
- [33] ALPHA, M. Guagnelli, R. Sommer and H. Wittig, Nucl. Phys. B535 (1998) 389, hep-lat/9806005.
- [34] R. Sommer, Nucl. Phys. B411 (1994) 839, hep-lat/9310022.
- [35] M. Lüscher and P. Weisz, Nucl. Phys. B479 (1996) 429, hep-lat/9606016.